RSC Advances

ROYAL SOCIETY OF CHEMISTRY

www.rsc.org/advances

Eye readable gasochromic and Optical Hydrogen Gas Sensor Based on CuS-Pd

Shankara S. Kalanur[1], Young-Ahn Lee[1], and Hyungtak Seo[1,2,*]

[1]Department of Energy Systems Research, Ajou University, Suwon 443-739, Republic of Korea

[2]Department of Materials Science and Engineering, Ajou University, Suwon 443-739, Republic of Korea

*Corresponding author: hseo@ajou.ac.kr

Abstract

Hydrogen gas sensing is a crucial issue in various hydrogen related areas due to its explosive nature. Here, we report an efficient gasochromic and optical hydrogen sensor based on ultrathin layer of copper sulfide (CuS) incorporated with palladium (Pd). When exposed to hydrogen environment, the CuS-Pd film changes color from dark green to brown which makes the proposed CuS-Pd an eye-readable sensor that circumvents the need for electronics, optic fiber and transducer or electrical readouts. The CuS-Pd can also be used as an optical sensor by taking the advantage of decrease in localized surface plasmon resonance in Infrared region, due to the reduction in free carrier density in CuS valence band upon exposure to H_2. CuS-Pd proposed optical sensor can efficiently detect the presence of upto 0.8% H_2 gas in air. Hence, CuS-Pd can be integrated into small size fiber optic devices as emerging new class of high-performance hydrogen gas sensors.

Introduction

Hydrogen (H_2) is regarded as one of the most promising clean-energy carriers of the future, with wide-range of applications in different fields like industrial processes, space application, biomedical, and fuel cells. The use of H_2 is expected to grow dramatically in the coming years due to the crucial role it can play as a backbone of future energy systems[1]. But, there is serious anxiety about safe production, storage, and usage because of its low ignition energy and wide flammable range which makes it easily inflammable and explosive[2]. H_2 is a low molecular weight gas and can easily leak out and may cause fires or explosions. Furthermore, H_2 gas is tasteless, colorless and odorless and hence, cannot be detected by human senses[3]. Therefore, H_2 leakage monitoring is extremely important. Making a robust, sensitive, and reliable H_2 sensing technology could facilitate commercial acceptance of hydrogen fuel in various applications.

Different types of H_2 sensors are reported, which exploit catalytic, electrochemical, mechanical, optical, acoustic, thermal conductivity, resistance and work-function related detection schemes[4-10]. Since H_2 detection often takes place in explosive environment, (for leak detection or hydrogen-concentration measurements in gas streams) the use of optical H_2 sensors has major advantage of being intrinsically safe due to the lack of electric contacts in the sensing area[3]. Therefore, optical monitoring of H_2 is considered less dangerous when compared to other techniques which require electric contacts. It offers additional advantage of remote, distributed and multiple H_2 sensing via optic fibers[1]. However, with all these advantages, the optical sensors still require a light source and electronic devices to convert the change in optical property into a readable output, which contributes considerably to the cost of the sensor and increased complexity. Therefore, fabricating a gasochromic sensor with eye-readable change in color is on demand to avoid the need for an optic fiber and transducer or electrical readout. Such a device may be applicable to instantaneous detection of H_2 leakage in diverse applications such as H_2 pipelines and in H_2 fuel cell automobiles.

So far, different materials like Y, WO_3, MoO_3, ZnO, TiO_2, SnO_2, In_2O_3 and graphene have been used for sensing H_2[1, 11-19]. Among them, WO_3, Y, and MoO_3 are used as gasochromic hydrogen sensors. However, gasochromic sensors based on WO_3, MoO_3, and Y are mostly reversible, expensive and need protective layers for longer life of working sensor. To the best of our knowledge, CuS has not been reported/used for hydrogen gas sensing applications till now. Copper sulfides, in particular covellite CuS is characterized by a strong free carrier absorption in near-infrared (NIR) region as a consequence of localized surface plasmon resonances (LSPR)[20,21]. Hence, LSPR absorption peak tends to change with the change in free carrier concentration. This LSPR characteristic of CuS is exploited in this study for sensitive gasochromic and optical H_2 sensor. Here, we demonstrate the fabrication of Pd coated CuS thin films on glass and flexible substrates and their application for gasochromic and optical sensor for the detection of H_2.

Experimental

Copper sulfide thin films were deposited on substrate (microscopic glass slides/flexible plastic sheet) using chemical bath deposition method. Copper sulfate was used as a source of copper and sodium thiosulphate as a sulfur source. The molar ratio of copper sulfate and sodium thiosulphate was maintained at 1:5. The transparent sheets of overhead projector (polyethylene terephthalate) were taken as flexible plastic substrates. Before the deposition, the substrate (glass/plastic) were cleaned and placed at an angle against the wall of the beaker containing 100 ml aqueous solution of 0.1 M copper sulfate and 0.5 M sodium thiosulphate. To deposit CuS on only one side of the substrate, the other side of the substrate was masked using 3M tape. The deposition was carried out at 65 ^{0}C for 135 minutes. After the deposition, the substrates were carefully washed and rinsed with water and dried in air. A thin

layer of Pd (thickness of 4 nm) was deposited on CuS thin films at room temperature using electron beam deposition technique.

To record the coloring/bleaching response of the CuS-Pd samples at 100% hydrogen, we used a sealed gas chamber. In order to investigate the coloring response at 1% hydrogen diluted 99% N_2 (in the background of air ambient; mixture of nitrogen, oxygen and water vapor) we used open chamber with outlet. All gasochromic experiments were carried out at room temperature with a flow rate of 2l min^{-1} over the CuS-Pd sample. The surface morphology and structural characterization of the CuS-Pd were probed using a Hitachi S4800 (Japan) scanning electron microscope (SEM) and a JEOL, JEM-2100F (USA) transmission electron microscope (TEM). EDS was measured with the instrument attached to TEM. X-ray diffraction (XRD) measurements were obtained on a MiniFlex desktop X-ray diffractometer instrument. UV–vis absorption spectra were recorded using a Varian Cary 5000 spectrophotometer (Australia). XPS analyses of the prepared films were carried out with a theta probe spectrometer using Thermo Fisher Scientific (USA).

Results and Discussion

The copper-sulfur system is reported to be complex one with several stable and metastable species occurring between Cu_2S (chalcocite) and CuS (covellite)[22]. During the synthesis of copper sulfide, the final product stoichiometry is dependent on stoichiometry between copper and sulfur precursor. Therefore, selective preparation of copper sulfide phases with their specific properties requires a precise adjustment of the relevant experimental conditions[22,23]. Here we deposit CuS thin films by reacting copper sulfate with sodium thiosulphate in molar ratio 1:5 (Fig. 1). Figure 2a illustrates the XRD pattern of as-prepared CuS thin films. It is evident from the XRD graph that the resultant product is of pure phase with no other peaks related to other copper sulfide species. The strong and sharp diffraction

peaks suggest that the obtained products are well crystalline in nature. The diffraction peaks of sample match well with the standard peaks of covellite CuS, JCPDS file no. 79-2321. For H_2 sensing, 4nm Pd is deposited on CuS thin films using electron beam deposition. The synthesized CuS-Pd is further characterized using TEM as shown in Figure 2b c and d. In higher resolution TEM image (Fig. 2b), the CuS nanoclusters with approximately 50 nm size are clearly seen. The size of the Pd nanoparticles on the surface of the CuS are approximately 4 to 5 nm. From Figure 2c and d, the interplanar d-spacing of 0.28 nm corresponding to the (1 0 3) lattice fringes, is assigned to hexagonal phase of covellite CuS single crystal and the interplanar d-spacing of 0.22 nm corresponding to the (1 1 1) lattice fringes, is assigned to cubic phase of Pd nanocrystal. The EDS spectra of CuS and CuS-Pd nanohybrid is shown in Figure S1. The top-view SEM (Fig. 2e) image of CuS thin film on glass reveals the uniform deposition of CuS on glass substrate (the SEM image of bare glass substrate is shown in inset Fig. 2e), covering the entire surface without any empty surface regions. The CuS thin layer deposited on glass exhibited good adhesion to the substrate. The good adhesion makes the films robust and stable for long term application. This shows the effectiveness and advantages of the present method in making uniform CuS thin films on glass. Figure 2f represents cross sectional SEM image of CuS-Pd thin film on glass with overall film thickness of ~50 nm. The inset in Fig. 2f represents top view SEM images of CuS-Pd thin films. However, Pd layer on CuS could not be visibly distinguished from SEM images due to small size/thickness.

Pure covellite CuS is characterized by a strong free carrier absorption in the NIR region[24-27], while the Cu_2S and other stoichiometric species does not show any absorption in that IR region. To investigate this, we performed UV-vis absorption measurements of fabricated CuS thin films in the wavelength range of 300-3000nm (Fig. S2). The synthesized covellite CuS thin films exhibited a well-defined NIR absorption peak, at around 1100 nm (Fig. S2). This peak is ascribable to in-plane LSPR mode, which dominates the plasmonic response[20]. This peak is in agreement with the previously reported absorption

spectra for pure covellite CuS[20] and confirms that the CuS thin films prepared in our study are the crystalline form of pure covellite CuS.

As prepared CuS films appeared semitransparent and dark green in color. Upon exposure to H_2 gas at room temperature, the color of the CuS-Pd film changed from dark green to brown. Inset in Figure 3a shows the camera image (without applying any image processing) of the CuS-Pd film on glass substrate before and after passing H_2 gas. In presence of 100% H_2 gas, complete change in coloration is observed, while only slight change in color is observed in 1% H_2 (equivalent to the true volume concentration of 0.8% H_2 in the reactor). The response time of CuS-Pd films in presence of 100% H_2 gas is noted to be less than 20 seconds and is less than 1 minute in presence of 1% hydrogen since H_2 flows begins (see supplementary video clip for real-time chemochromic response). The present procedure was further applied to deposit CuS thin films on flexible plastic substrates (Fig. 4a). Figure 4b shows the camera image of CuS-Pd film on flexible substrate (OHP sheet) before and after passing H_2. Significant change in color is observed after passing H_2 gas. This shows additional application of the proposed synthesis method for the fabrication of flexible gasochromic sensors.

Covellite CuS has strong p-type metallic character with the highest concentration of free carriers in the copper sulfide class of materials. Therefore, covellite CuS are particularly characterized by strong free carrier absorption in the NIR region (Fig. S2). CuS have a hole density of about 10^{21} cm^{-3} which sets their LSPR energy in the NIR range. While in case of stoichiometric Cu_2S, the valence band is completely filled and thus does not show absorption in the NIR region. Hence, LSPR absorption peak tends to change with the change in free carrier concentration. Figure 3b and c depicts absorption spectra of CuS-Pd thin films on glass in presence and absence of H_2 gas in the wavelength range 300-3000 nm. It is clear from the absorption spectra of CuS-Pd that, significant decrease in absorbance is observed in the wavelength range of 1100-2500 nm after passing H_2 gas. This decrease in LSPR is attributed to the

decrease in hole density at the valence band CuS system (Fig. 3a). This optical property is similar to that of Cu_2S in which valence band is completely filled and thus does not show LSPR peak in the NIR range.

Figure S3a and S3b, represents transmittance spectra of CuS-Pd thin films in presence and absence of 100% and 0.8% hydrogen in the wavelength range 300-3000 nm. Significant change in transmittance spectra is observed after passing 100% and 0.8% H_2 gas. This shows the sensitivity of the CuS-Pd sensor towards hydrogen gas. Therefore, most promising optical H_2 sensor can be fabricated using CuS-Pd which operates in transmittance mode using plastic collimating lenses. The absorption and transmittance spectra of CuS-Pd thin films on OHP sheet in presence and absence of hydrogen in the wavelength range 300-3000 nm are shown in Figure 4c and 4d. Significant change in absorption and transmittance spectra are observed after exposing to hydrogen gas shows additional application as flexible H_2 sensors. The change in color or optical properties of CuS-Pd thin films on H_2 exposure is noted to be dependent on time. Figure S4 shows response time of the sensor at different H_2 gas concentration. The sensitivity of the proposed CUS-Pd sensor was compared with other materials reported for gasochromic and optical H_2 sensors. Table 1 summarizes the detection sensitivity of the present method with the reported hydrogen sensors.

Based on our experimental results and observations, we proposed a probable H_2 sensing mechanism of CuS-Pd. When CuS-Pd thin film is exposed to H_2 gas, H_2 molecules get absorbed on Pd which are then dissociate into hydrogen atoms on the surface of Pd. These dissociated hydrogen atoms may transfer onto the surfaces of CuS layer by spillover and are injected into the bodies of CuS there by reducing hole density in the valence band of CuS. This was evident from the significant decrease LSPR peak at NIR shown in Figure 4c and 4d. To identify the chemical status of Cu element in the samples, X-ray photoelectron spectroscopy (XPS) analysis was carried out. Figure 5a shows XPS of Cu profile samples before and after passing H_2 gas. The shakeup line in XPS of Cu element between 943-945 and an asymmetric tail (Black line in Fig. 5), already known for covellite CuS, represents the density of free holes

in CuS[20, 28]. This asymmetric tail was gradually reduced in the samples after passing H_2 (Red line in Fig. 5), this reveals the decrease in the density of free holes of CuS valence band[20] in agreement with the absorbance data of CuS-Pd before and after passing H_2 gas. It has been reported that, hydrogen strongly affects the electronic and structural properties of materials by binding to anions/cations (in semiconductors) or defects or to other impurities[29]. According to Van de Walle et al.,[29] hydrogen exhibits qualitatively different behavior depending on the host into which it is introduced. That is, it can act as either a donor (H^+) or an acceptor (H^-) depending on the material. In particular, when hydrogen gas is introduced into semiconductors, hydrogen bonds to the anionic species in p-type material, and to the cationic species in n-type material[29]. Since CuS is a p-type semiconductor, it can be concluded that the hydrogen is assumed to bind to sulfide species in CuS-Pd system. In CuS, the top of the valence band has a strong contribution from the sulfur p orbitals and the bottom of the conduction band has mainly contributions from Cu 4s and 4p orbitals[30]. Therefore, hydrogen binding to sulfide species mainly effects valence band of CuS system. This is in agreement with the absorbance and XPS data of Cu that the hole density at the valence band of CuS is mainly affected in presence of hydrogen which is contributed from sulfur. Interesting changes were also observed in the S 2p region of the XPS. Typical S 2p binding state (Figure 5b, black curve) in covellite CuS is characterized by the "three peaks"[20]. Deconvolution to subcomponents (Fig. S5) revealed the presence of two main doublets, which are characteristic of sulfide moiety at binding energy of 161.5 ± 0.1 eV (peak 1 in Fig. S5a) and disulfide moiety at 162.3 ± 0.1 eV (peak 2 in Fig. S5a) in covellite. After hydrogen gas exposure, the intensity ratio between the disulfide and the sulfide components gradually decreased. That is, the peak intensity of sulfide moiety at 161.5 (peak 1 in Fig. S5b) increased while that of disulfide moiety at 162.3 (peak 2 in Fig. S5b) decreased. This indicates that the average −1 valence of S of covellite gradually evolved to −2[20] after passing hydrogen. Based on our results a probable sensing mechanism is proposed as shown in Figure 5c.

The eye-readable H_2 chemochromic effect in CuS-Pd is irreversible or does not recover with time in air. This ensures CuS as a discriminated class of H_2 chemochromic materials from all other oxide-based materials, which are reversible due to oxygen re-adsorption in air. It will be greatly useful for the first-level H_2 leakage detection, for example, in the massive H_2 delivery pipe line. We investigated the stability of the CuS-Pd samples over a period of 5 months. To test this, 5 set of samples were prepared and tested for chemochromic effect at different days. The samples were kept in open air at lab atmosphere. When exposed to H_2 gas, the films showed appreciable change in color (dark green to brown) which was observed to be irreversible over the period tested (Fig. S6). In addition, the stability of CuS-Pd bonding was again tested by measuring TEM after hydrogen exposure. Fig. S7 illustrates TEM of CuS-Pd system after hydrogen exposure which shows significant binding even after hydrogen exposure. In order to test the selectivity of the CuS-Pd thin films in hydrogen sensing applications, we carried out selectivity experiments in presence of CO and methane gases. Fig. S8 shows the photographic image and optical characteristics of CuS-Pd thin films in presence of CO and methane gases. CuS-Pd thin films did not show any visible change in color or absorbance or transmittance in presence of only CO and methane gas. However, H_2 sensing properties of CuS-Pd thin films were noticed to be changed in presence of CO and methane (fig. S8). In presence of CO, the H_2 sensing properties are noticed to be decreased while in presence of methane gas the sensing property is enhanced. Therefore, although individually CO or methane did not react with CuS, it is suggested that these gases may affect the H_2 adsorbing property of Pd nanoparticle. The change in color and optical properties in CuS-Pd thin films in presence of CO, methane and H_2 indicates good selectivity of the proposed sensor.

Conclusions

An efficient and cost effective chemochromic and optical H_2 sensor has been introduced based on CuS-Pd thin film. The change in the color/optical properties of the CuS-Pd nanostructured thin films

upon exposure to H_2 allows us to create eye-visible effects, making it new gasochromic sensor in this class. Based on our experimental results, it was concluded that H_2 gas interacts and binds with sulfur in CuS-Pd system, thereby decreasing the hole density at CuS valence band which in turn effects its LSPR property of CuS. The proposed gasochromic CuS-Pd film can detect upto 0.8% H_2 gas in air. In addition, the present method for the deposition of CuS thin films on glass/flexible plastic makes the proposed technique cost effective and feasible for the large scale production. The present work also opens new possibilities of using copper sulfide based materials for H_2 sensing applications.

Acknowledgements

This work was supported by Hyundai Motors Industry-University Research Program, the Basic Science Program (NRF-2012R1A1A1005014) through the National Research Foundation (NRF) of funded by MEST, ICT and Future Planning, Republic of Korea, and by the Basic Science Program (NRF-2009-0094046) through NRF funded by the Ministry of Education, Republic of Korea. Postdoctoral Fellowship to S.K. was funded by BK-plus programme.

Notes and References

Electronic Supplementary Information (ESI) available: [SEM-EDS data, UV-vis spectra, XPS data with peak deconvolution, sensor aging test results, and video clip for the real time sensing performance]. See DOI: 10.1039/b000000x/

References

1. N. Peter, R. Tsveta, S. Martin, J. W. Ruud, S. Herman and D. Bernard, Adv. Funct. Mater., 2014, **24**, 2374-2382.
2. K. J. Liekhus, I. A. Zlochower, K. L. Cashdollar, S. M. Djordjevic and C. A. Loehr, *J. Loss Prev. Process Ind.*, 2000, **13**, 377-384.
3. P. A. Szilagyi, R. J. Westerwaal, R. van de Krol, H. Geerlings and B. Dam, *J. Mater. Chem. C* 2013, **1,** 8146-8155.
4. T. Hübert, L. Boon-Brett, G. Black and U. Banach, *Sens. Actuators B* 2011, **157,** 329-352.
5. X. Q. Zeng, Y. L. Wang, H.Deng, M. L. Latimer, Z. L. Xiao, J. Pearson, T. Xu, H. H. Wang, U. Welp, G. W. Crabtree and W. K. Kwok, *ACS Nano* 2011, **5**, 7443-7452.
6. J. Lee, W. Shim, E. Lee, J. S. Noh and W. Lee, *Angew. Chem. Int. Ed.*, 2011, **50**, 5301-5305.
7. C. McDonagh, C. S. Burke and B. D. MacCraith, *Chem. Rev.*, 2008, **108,** 400-422.
8. R. R. J. Maier, B. J. S. Jones, J. S. Barton, S. McCulloch, T. Allsop, J. D. C. Jones abd I. Bennion, *J. Opt. A: Pure Appl. Opt.*, 2007, **9,** S45.
9. C. Perrotton, N. Javahiraly, M. Slaman, B. Dam and P. Meyrueis, *Opt. Express* 2011, **19,** A1175-A1183.
10. M. A. Butler, *Appl. Phys. Lett.*, 1984, **45**, 1007-1009.
11. M. Yang, Z. Yang, J. Dai and D. Zhang, *Sens. Actuators B,* 2012, **166-167,** 632-636.
12. M. H. Yaacob, J. Yu, K. Latham, K. Kalantar-zadeh and W. Wlodarski, *Sens. Lett.*, 2011, **9**, 16-20(15).
13. R. Yatskiva, J. Gryma, K. Zdanskya and K. Piksovab, *Carbon,* 2012, **50**, 3928-3933.
14. J. Lee, D. H. Kim, S. Hong and J. Y. Jho, *Sens. Actuators B,* 2011, **160,** 1494-1498.
15. Z. Wang, Z. Li, T. Jiang, X. Xu and C. Wang, *ACS Appl. Mater. Interfaces,* 2013, **5**, 2013-2021.
16. H. Huang, H. Gong, C. L. Chow, J. Guo, T. John-White, M. S. Tse and O. K. Tan, *Adv. Funct. Mater.*, 2011, **21,** 2680-2686.
17. A. Kumara, P. Zhang, A. Vincenta, R. McCormack, R. Kalyanaramane, H. J. Cho and S. Seala, *Sens. Actuators B,* 2011, **155,** 884-892.
18. U. Lange, T. Hirsch, V. M. Mirsky and O. S. Wolfbeis, *Electrochim. Acta,* 2011, **56,** 3707-3712.
19. A. R. Patrícia, D. Nicola, G. L. Salvatore, B. Seunghwan, E. C. Donato, N. Giovanni and P. Nicola, *Angew. Chem. Int. Ed.*, 2012, **51**, 11053-11057.
20. Y. Xie, A. Riedinger, M. Prato, A. Casu, A. Genovese, P. Guardia, S. Sottini, C. Sangregorio, K. Miszta, S. Ghosh, T. Pellegrino and L. Manna, *J. Am. Chem. Soc.*, 2013, **135,** 17630-17637.
21. Y. Zhao, H. Pan, Y. Lou, X. Qiu, J-J, Zhu and C. Burda, *J. Am. Chem. Soc.*, 2009, **131**, 4253–4261.
22. M. D. Kate, G. Franz and W. H. Thomas, *Langmuir,* 1999, **15**, 6637-6642.
23. C. M. Simonescu, l. Patron, V. S. Teodorescu, M. Brezeanu and C. Capatina, *J. Optoelectron. Adv. M.*, 2006, **8**, 597-600.
24. M. C. Brelle, C. L. Torres-Martinez, J. C. McNulty, R. K. Mehra and J. Z. Zhang, *Pure Appl. Chem.*, 2000, **72,** 101-117.
25. E. J. Silvester, F. Grieser, B. A. Sexton and T. W. Healy, *Langmuir,* 1991, **7,** 2917-2922.
26. I. Grozdanov and M. Najdoski, *J. Sol. St. Chem.*, 1995, **114**, 469-475.
27. K. V. Yumashev, P. V. Prokoshin, A. M. Malyarevich, V. P. Mikhailov, M. V. Artemyev and V. S. Gurin, *Appl. Phys. B: Lasers Opt.*, 1997, **B64,** 73-78.
28. J. Ghijsen, L. H. Tjeng, J. van Elp, H. Eskes, J. Westerink, G. A. Sawatzky and M. T.Czyzyk, *Phys. Rev. B*, 1988, **38**, 11322–11330.
29. C. G. Van de Walle and J. Neugebauer, *Lett to Nature*, 2003, **423**, 626-628.

30. E. J. D. Garba and R. L. Jacobs, *Physica B+C*, 1986, **138**, 253-260.
31. M. E. Nasir, W. Dickson, G. A. Wurtz, W. P. Wardley and A. V. Zayats, *Adv Mater*. 2014, **4**, 3532-3537.
32. T. Radeva, P. Ngene, M. Slaman, R. Westerwaal, H. Schreuders and B. Dam, *Sens. Actuators B,* **203**, 2014, 745–751.
33. W-L. Jang, Y-M. Lu, Y-R. Lu, C-L. Chen, C-L. Dong, W-C. Chou, J-L. Chen, T-S. Chan, J-F. Lee, C-W. Pao and W-S. Hwang, *Thin Solid Films*, 2013, **544**, 448–451.
34. B. Orel, N. Grošelj, U.Opara Krašovec, M. Gabrščček, P. Bukovec and R. Reisfeld, *Sens. Actuators B,* **1998**, 50, 234–245.

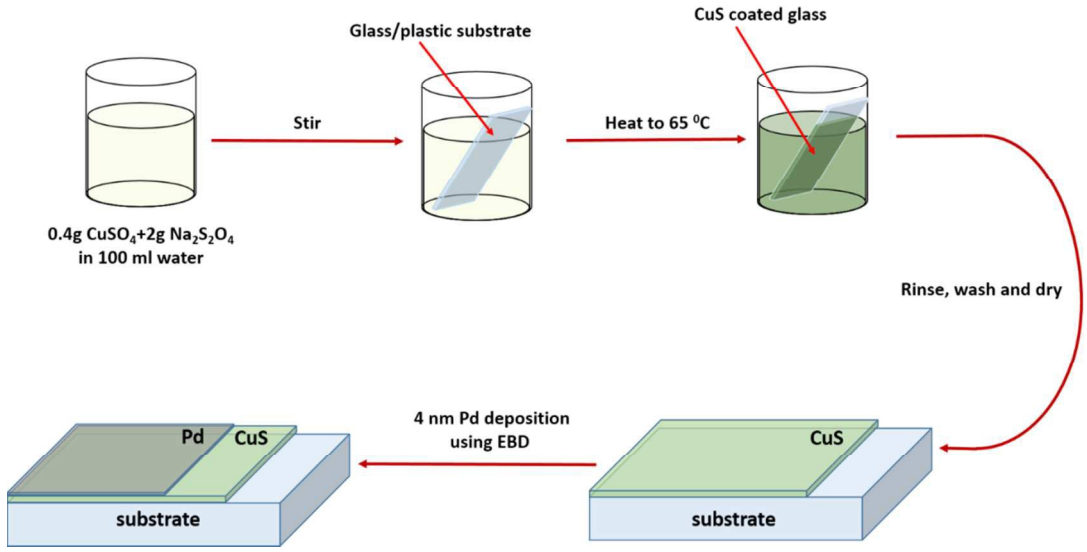

Figure 1. Fabrication procedure of CuS-Pd nanohybrid thin film.

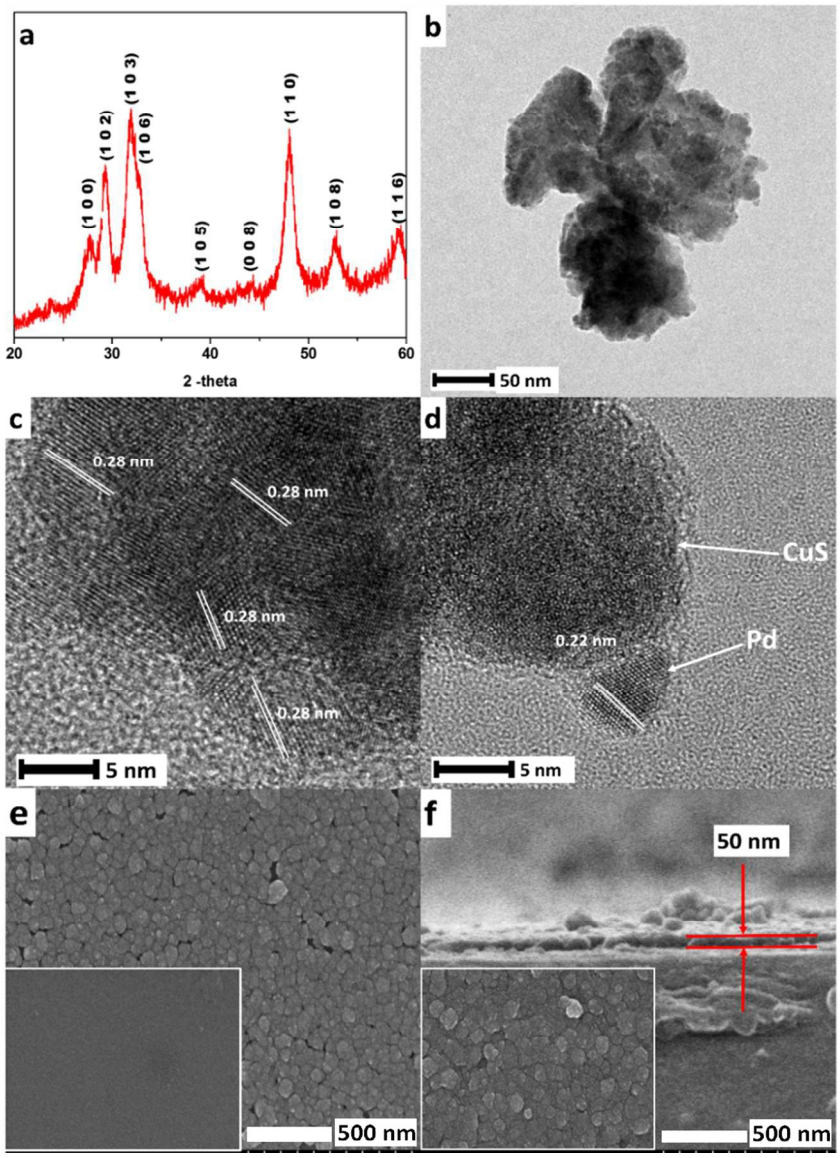

Figure 2. (a) XRD pattern of the covellite CuS (JCPDS card 79-2321). (b) TEM image of CuS-Pd nanohybrid. (c) and (d) are the lattice-resolved TEM images of CuS and CuS-Pd, respectively. Interplanar d-spacings of 0.28 nm in (in c) corresponds to the (1 0 3) lattice fringes of covellite CuS and 0.22 nm in (in d) corresponds to (1 1 1) lattice fringes of Pd. (e) Top view SEM image of CuS thin film on glass and its inset shows SEM image of bare glass surface. (f) corss-sectional SEM image CuS-Pd thin film (50nm) on glass and its inset shows the surface of CuS-Pd thin film on glass.

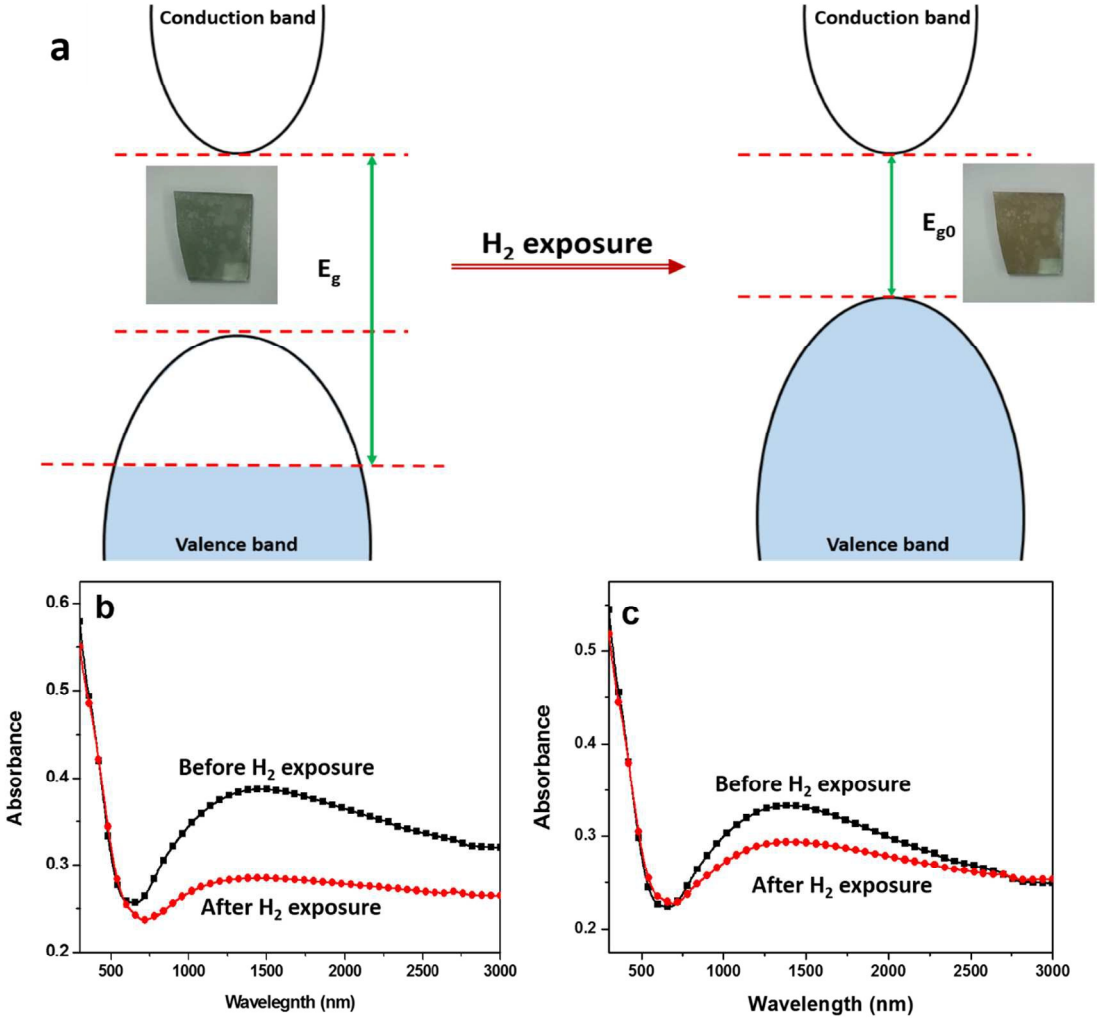

Figure 3. (a) Band diagram of CuS-Pd system before and after passing hydrogen gas. Insets camera images show the change in color of CuS-Pd films before and after passing hydrogen (dark green to brown). Absorbance of CuS-Pd films before (black line) and after (red line) passing (b) 100 % and (c) 0.8 % hydrogen gas.

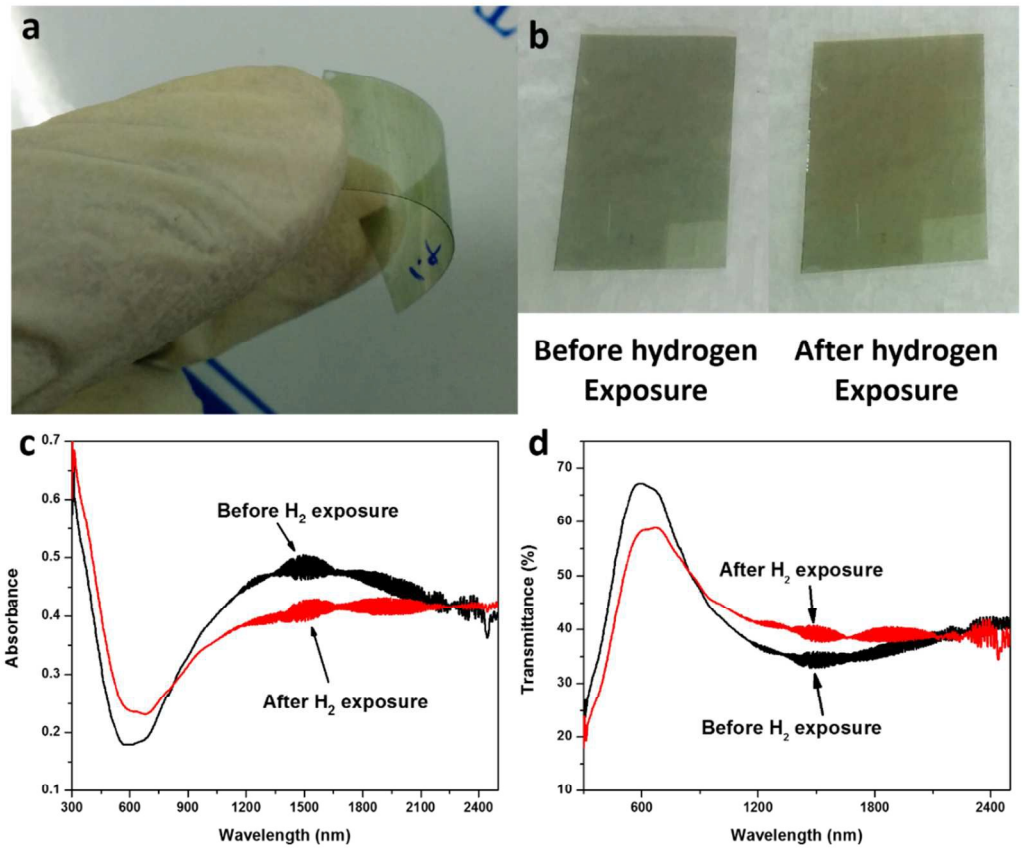

Figure 4. (a) Camera image of CuS thin films on flexible plastic substrate (OHP sheet). (b) Camera image of CuS-Pd nanohybrid on OHP sheet before and after passing hydrogen. (c) Absorbance and (d) transmittance spectra of CuS-Pd nanohybrid before and after passing hydrogen.

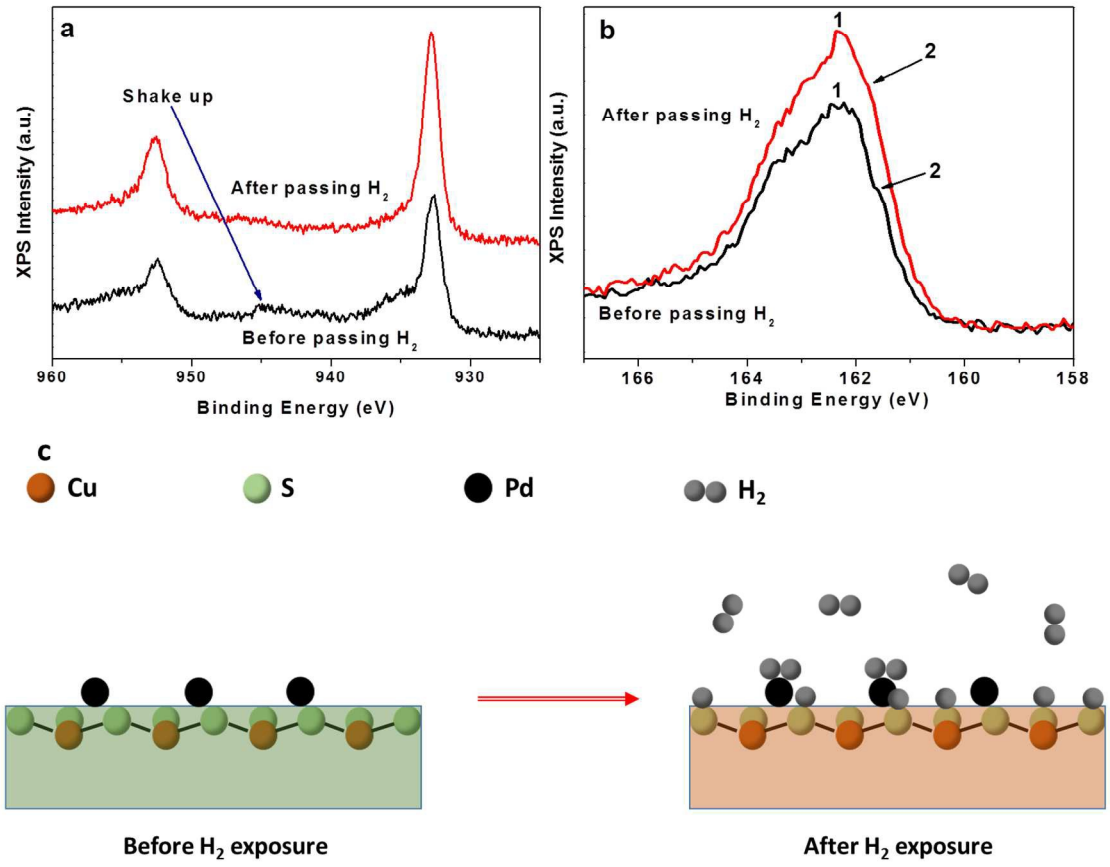

Figure 5. High resolution XPS characterization of CuS-Pd nanohybrid films on glass in (a) Cu 2p region and (b) S 2p region. (c) Probable hydrogen sensing mechanism of CuS-Pd nanohybrid film.

Table 1 Reported gasochromic/optical hydrogen sensors and their sensitivity compared to the present study

Material	Type of sensor	Sensitivity/hydrogen detection limit	Reference
Y	Gasochromic/optical	0.1% H_2	1
Au-Pd	Gasochromic/optical	2% H_2	31
Y–Mg alloys	Gasochromic/optical	0.25% H_2	32
V_2O_5	Gasochromic	10% H_2	33
palladium doped Peroxopolytungstic acid	Gasochromic	4% H_2	34
CuS-Pd	Gasochromic/optical	0.8% H_2	Present study